



Role of ambient ammonia in particulate ammonium formation at a rural site in the North China Plain

Zhaoyang Meng¹, Xiaobin Xu¹, Weili Lin², Yulin Xie^{3,4}, Bo Song³, Shihui Jia^{1,5}, Rui Zhang^{6,7}, Wei Peng¹, Ying Wang¹, Hongbin Cheng¹, Wen Yang⁵, Huarong Zhao¹

5

¹ State Key Laboratory of Severe Weather & Key Laboratory for Atmospheric Chemistry of CMA, Chinese Academy of Meteorological Sciences, Beijing 100081, China

² CMA Meteorological Observation Centre, Beijing 100081, China

³ University of Science and Technology Beijing, Beijing 100083, China

10 ⁴ Baotou Steel Group Mining Research Institute, Baotou 014010, China

⁵ South China University of Technology, Guangzhou 510641, China

⁶ Chinese Research Academy of Environmental Sciences, Beijing 100012, China

⁷ Beijing Municipal Research Institute of Environmental Protection, Beijing 100037, China

15 *Correspondence to:* Zhaoyang Meng (mengzy@camsma.cn)

Abstract. The real-time measurements of NH₃ and trace gases were conducted, in conjunction with semi-continuous measurements of water-soluble ions in PM_{2.5} at a rural site in the North China Plain (NCP) from May to September 2013 in order to better understand of chemical characteristics for
20 ammonia, and of the impact on formation of secondary ammonium aerosols in the NCP. Extremely high NH₃ and NH₄⁺ concentrations were observed after a precipitation event within 7-10 days following urea application. Elevated NH₃ levels coincided with elevated NH₄⁺, suggesting that NH₃ plays a vital role in enhancing particulate ammonium. For the sampling period, the average oxidation/conversion ratios for SO₄²⁻ (SOR), NO₃⁻ (NOR) and NH₄⁺ (NHR) were estimated to be 64%, 24% and 30%,
25 respectively. The increased NH₃ concentrations mainly from agricultural activities, coincided with the prevailing meteorological conditions could promote the secondary transformation, resulting in higher hourly SOR, NOR and NHR. The concentrations of NH₃, NH₄⁺, and NHR had clear diurnal variations, which could be attributed to their sources, meteorological conditions, and formation mechanisms. The back trajectory analysis indicates that the transport of air masses from the North China Plain region
30 contributed to the atmospheric NH₃ variations, and both regional sources and long-distance transport from southeast played important roles in the observed ammonium aerosol at rural site in the NCP. The findings of this study are expected to facilitate developing future NH₃ emission control policies for the North China Plain.



Keywords: Ambient ammonia; ammonium in PM_{2.5}; the conversion ratio of NH₄⁺; agricultural activity; North China Plain.

1 Introduction

5 Ammonia (NH₃) is a very important alkaline constituent in the atmosphere, plays an important role in atmospheric chemistry and is closely related to ecosystems. NH₃ has both direct and indirect impacts on critical environmental issues, including regional fine particles, acid rain, and eutrophication (Roelle and Aneja, 2002; Krupa, 2003; Reche et al., 2012). In addition, NH₃ is a key species for neutralising H₂SO₄ and HNO₃ in the atmosphere and forming (NH₄)₂SO₄, NH₄HSO₄, and NH₄NO₃ (Erisman and
10 Schaap, 2004; Walker et al., 2004), which are major components of fine particulate matters and contribute to regional haze (Ye et al., 2011; Meng et al., 2014; Wei et al., 2015). Global ammonia emission has more than doubled since pre-industrial times, mainly because of agricultural intensification (Galloway et al., 2015). The total ammonia emission in China in 2006 was estimated to be 16.07 million tons (Mt) (Dong et al., 2015). Such high emission makes NH₃ one of the key species
15 related to atmospheric environmental problems. Many studies have indicated that ammonia is a crucial precursor in the formation of fine particles (Cao et al., 2009; Wu et al., 2009; Meng et al., 2011; Shen et al., 2011; Park et al., 2014; Wang et al., 2015).

As global food production requirements increase, agriculture plays an increasingly important role in local, regional, and global air quality (Walker et al., 2006). The North China Plain (NCP) is a highly
20 populated region with intensive agricultural production as well as heavy industry. The region has been affected by severe haze and photochemical pollution in recent years (Guo et al., 2010; Wang et al., 2010; Luo et al., 2013). Covering only 3.3% of the national area, the NCP region provides 40% and 25% of China's wheat and corn production. To sustain such high agricultural productivity, chemical fertilisers have been intensively applied. Less than 30% efficiency in N application causes
25 approximately 40% N loss through various routes including the leaching of NO₃⁻ and emission of NH₃, N₂O, and N₂ (Zhang et al., 2010). So far, only a few limited studies have paid attentions to impacts of NH₃ on air pollution in the NCP region. According to some studies (Dong et al., 2010; Ianniello et al., 2010; Meng et al., 2011; Shen et al., 2011; Meng et al., 2015), the high NH₃ emission intensities observed in the NCP have been caused by high fertiliser application rates and numerous intensive



livestock farms. However there were few simultaneous high time resolution measurements of NH_3 and NH_4^+ in $\text{PM}_{2.5}$, and investigating the role in fine particulate formation in China. These studies are necessary to improve our understanding of ammonia pollution on regional air quality, and of the impact on formation of secondary ammonium aerosols in the NCP.

5 During May–September 2013, the intensive field measurements of NH_3 and other trace gases, water-soluble ions in $\text{PM}_{2.5}$, and meteorological parameters took place at a rural site in the NCP. In this article, we report the results on NH_3 , trace gases and major water-soluble ions in $\text{PM}_{2.5}$. We discuss temporal variations and diurnal patterns of NH_3 and NH_4^+ , and examine their sources and chemical conversion mechanism.

10 2 Description of Experiment

2.1 Measurement site

The measurements were performed from May to September 2013 at Gucheng (39°08'N, 115°40'E, 15.2 m a.s.l.), a rural site in the NCP, which is an Integrated Ecological Meteorological Observation and Experiment Station of the Chinese Academy of Meteorological Sciences. In Fig. 1, the location of the site is shown on the NCP map with the NH_3 emission distribution for the year 2012 from the multi-resolution emission inventory of China (<http://meicmodel.org/index.html>). The measurement site chosen is situated for monitoring regional background concentrations of air pollutants in the North China Plain, has good regional representativeness (Lin et al., 2009). The site is approximately 110 km southwest of Beijing, 130 km west of Tianjin, and 160 km northeast of Shijiazhuang City in Hebei Province. The site is surrounded by farms, dense villages, and transportation networks. The main crops in the area surrounding the site are wheat (winter and spring) and corn (summer and fall). The site is influenced by high NH_3 emissions from fertiliser use and animal husbandry in the surrounding area. Being in the warm temperate zone, the site has a typical temperate continental monsoon climate. Precipitation occurs mainly between May to August.

25 2.2 Sampling and analysis

Ambient NH_3 was measured using an ammonia analyser (DLT-100, Los Gatos Research, USA), which utilize a unique laser absorption technology called Off-Axis Integrated Cavity Output Spectroscopy (OA-ICOS). The analyzer has a precision of 0.2 ppb at 100 sec average and a maximum drift of 0.2 ppb over 24 hrs. During the campaign, NH_3 data were recorded as 50-s average. A set of commercial instruments from Thermo Environmental Instruments, Inc. was used to measure O_3 (TE 49C),



NO/NO₂/NO_x (TE 42CTL), CO (TE 48C), and SO₂ (TE 43CTL). All instruments were housed in an air-conditioned room in the observation building at the Gucheng site. Two parallel inlet tubes (Teflon, 4.8 mm ID×8 m length) were shared by the analyzers. The height of the inlets was 1.8 m above the roof of the building and about 8m above the ground. The inlet residence time was estimated to be less than 5 s.

In principle, the NH₃ analyzer does not need external calibration, because the measured fractional absorption of light at an ammonia resonant wavelength is an absolute measurement of the ammonia density in the cell (Manual of Economical Ammonia Analyzer - Benchtop Model 908-0016, Los Gatos Research). However, we calibrated the NH₃ analyzer using a reference gas mixture NH₃/N₂ (Scottgas, USA) to avoid potential drifts caused fine particles that may not be completely removed from the sample gas. During calibration, a sequence with 5 points of different NH₃ concentrations (including zero) were repeated overnight. Because of its absorbability, the duration time of each point was set to 3 hr for a fully stabilizations. Zero and span checks of other trace gases were performed weekly to identify possible analyser malfunctions and zero drifts. Multipoint calibrations of SO₂, NO_x, CO and O₃ analysers were performed on the instruments at approximately 1-month intervals. After the correction of data on the basis of the multipoint calibrations, hourly average data were calculated and used for the analysis.

An Ambient Ion Monitor (AIM) (URG 9000D Series, USA) was deployed at the site to measure hourly concentrations of water-soluble inorganic components in PM_{2.5} during 15 June–11 August, 2013. The detection limit of the AIM is 0.1 μg m⁻³ for various ionic components. For the AIM, multipoint calibrations were performed weekly by using calibration standard solutions. Acceptable linearity of ions was obtained with an R² of ≥0.999. The flow rate of the AIM was maintained at 3 L min⁻¹ and checked weekly at the sample inlet. Hourly data were obtained for the concentrations of water-soluble inorganic ions.

Meteorological data, including wind, temperature, and RH, were also obtained from the site, with a resolution of 1 hour.

2.3 Data analysis

2.3.1 Chemical conversions of species

Sulfate and nitrate oxidation ratios (SOR and NOR) are defined as the molar ratio of SO₄²⁻ and NO₃⁻ in PM_{2.5} to the total oxidized S and N, respectively (Zhang et al., 2011).



$$\text{SOR} = \frac{\text{SO}_4^{2-}}{\text{SO}_4^{2-} + \text{SO}_2} \quad (1)$$

$$\text{NOR} = \frac{\text{NO}_3^-}{\text{NO}_3^- + \text{NO}_x} \quad (2)$$

Similarly, the conversion ratio of ammonium (NHR) is expressed in terms of the ratio of ammonium to total ammonia (NH_x), which could be a measure of the extent of transformation from NH_3 to NH_4^+ in areas with major local NH_3 sources (Hu et al., 2014).

$$\text{NHR} = \frac{\text{NH}_4^+}{\text{NH}_4^+ + \text{NH}_3} \quad (3)$$

2.3.2 Trajectory calculation

The 72-h backward trajectories were calculated using the HYSPLIT 4.9 model (<http://www.arl.noaa.gov/ready/hysplit4.html>). The trajectories terminated on a height of 100 m above the ground. The trajectory calculations were done for four times (00:00, 06:00, 12:00, and 18:00 UTC) per day in summer 2013. The various back trajectories were grouped into five clusters. The number of clusters is identified according to the changes of total spatial variance (TSV). Five is chosen as the final number of clusters considering optimum separation of trajectories (larger number of clusters) and simplicity of display (lower number of cluster). The corresponding concentrations of trace gases and water soluble ions were averaged over the period of 3 h ahead and after the arrival time for each backward trajectory for further analysis.

3 Results and discussion

3.1 Overview of concentration levels of measured species

During 15 May–25 September 2013, the average concentrations of NH_3 , SO_2 and NO_x were 36.2 ± 56.4 , 5.0 ± 6.5 and 15.4 ± 9.3 ppb, respectively. As listed in Table 1, the concentration of NH_3 at the NCP rural site was lower than those reported in Asian and Africa urban sites such as Lahore (Pakistan) (Biswas et al., 2009), Colonelganj (India) (Behera et al., 2010) and Cairo (Egypt) (Hassan et al., 2013), but higher than those from other areas in China, Europe and North American (Plessow et al., 2005; Yao et al., 2006; Lin et al., 2006; Walker et al., 2006; Hu et al., 2008; Meng et al., 2011; Shen et al., 2011; Schaap et al., 2011; Makkonen et al., 2012; Behera et al., 2013; Gong et al., 2013; Meng et al., 2014; Li et al., 2014). For example, the NH_3 at the NCP rural site was higher than those found at Shangdianzi regional background station in the NCP (Meng et al., 2011), Lin'an regional background station in the Yangtze



River Delta (YRD) in Eastern China (Meng et al., 2014) and the rural site in Beijing (Shen et al., 2011). The relatively high concentrations of NH_3 observed in this study were attributed to agricultural activities involving fertiliser use, vegetation, and livestock, as well as human activity in the surrounding region.

5 According to an inventory study (Zhng et al., 2010), the total agricultural $\text{NH}_3\text{-N}$ emission in 2004 in the NCP was 3071 kt yr^{-1} , accounting for 27% of the total emissions in China with the 1620 kt yr^{-1} of $\text{NH}_3\text{-N}$ emissions caused by fertiliser applications, which is the largest emission source accounting for more than half of the total agricultural emissions. Our results are expected to be used in improving NH_3 emission inventory and making future emission control policies.

10 The observed concentration of SO_2 at the NCP rural site was markedly lower than those reported for the same period in 2006–2007 (Lin et al., 2009). Because of a series of emission reduction measures implemented in recent years, SO_2 levels have decreased markedly in the NCP (Lin et al., 2011). The average concentration of NO_x was higher than those at Shangdianzi (Meng et al., 2011) and Lin'an (Meng et al., 2014) regional background stations in the NCP and YRD region of China, which might be
15 due to emission from agricultural activities and motor vehicle sources (Liu et al., 2013; Lei and Wuebbles, 2013) in the NCP, but was lower than those at urban sites in India (Behera et al., 2010) and Egypt (Hassan et al., 2013).

The average concentrations of NH_4^+ , SO_4^{2-} , and NO_3^- in $\text{PM}_{2.5}$ were 19.8 ± 33.2 , 20.5 ± 13.6 and $11.3 \pm 9.1 \mu\text{g m}^{-3}$, respectively, at the NCP rural site during 15 June–11 August 2013. The average
20 concentration of NH_4^+ in $\text{PM}_{2.5}$ was higher than those observed at the rural or urban sites in the NCP (Meng et al., 2011), YRD (Meng et al., 2014), Beijing (Shen et al., 2011), Guangzhou (Hu et al., 2008), and Hong Kong (Yao et al., 2006) in China, and comparable to that at urban site in India (Behera et al., 2010). The average concentration of SO_4^{2-} in $\text{PM}_{2.5}$ was higher than those at rural sites in the NCP (Meng et al., 2011) and YRD (Meng et al., 2014) in China, but was lower than that observed at rural
25 sites in Guangzhou (Hu et al., 2008) in China, as well as urban sites in India (Behera et al., 2010) and Egypt (Hassan et al., 2013). The average concentration of NO_3^- in $\text{PM}_{2.5}$ was higher than those observed at the rural sites in the YRD and Guangzhou (Hu et al., 2008) in China, and lower than those at urban sites in India (Behera et al., 2010) and Pakistan (Biswas et al., 2008). The elevated NH_3 and NH_4^+ in $\text{PM}_{2.5}$ concentrations at the NCP rural site demonstrate severe ammonia and fine particulate
30 ammonium pollution in this area.



3.2 Ambient ammonia

3.2.1 Temporal variation of NH₃

The time series of hourly averages of NH₃ and other trace gases together with meteorological parameters during 15 May–25 September 2013 are shown in Fig. 2. NH₃ concentrations varied considerably during the observation period, ranging from 0.12 to 862.9 ppb. The NH₃ concentration increased rapidly on the seventh day after the urea application on 20 July, peaking during the 27–30 July period. The highest hourly value of NH₃ (862.9 ppb) was observed at 04:00 local time on 29 July 2013, with the second highest concentration observed at 06:00 on the same day. The extremely high NH₃ concentrations were probably caused by intensified soil emissions after rainfall on 26 July, which enhanced the soil moisture. Precipitation and the resulting soil water dynamics are known to strongly affect urea hydrolysis and subsequent NH₃ emissions (Reynold and Wolf, 1987; Aranibar et al., 2004). The general increase in NH₃ emissions was observed when soils with high moisture content began to dry because of increased diffusion (Burch et al., 1989). In addition, high temperatures promote NH₃ volatilisation from urea and ammonium dibasic phosphate applied to crops.

The monthly concentration of NH₃ depends on its source and meteorological conditions. The monthly average values of NH₃ were 28.4, 73.9, 26.4, and 13.5 ppb in June, July, August, and September 2013, respectively. In summer, high temperature promotes the emission of NH₃ from natural and fertilised soils, as well as vegetation. The concentration of NH₃ in July was approximately five times higher than that in September, which was influenced by higher temperature and increased emission rates of local agricultural NH₃ sources in July.

SO₂ and NO_x are the main precursors of sulfate and nitrate aerosols, and O₃ play an important role in atmospheric chemistry because they act as sources of OH radicals through photolysis. The maximum hourly average concentrations of SO₂ and NO_x were 86.8 ppb at 00:00 on 21 May and 67.7 ppb at 10:00 on 17 September, respectively. O₃ monthly levels were high in June (44.3 ppb) and July (43.7 ppb), with a maximum hourly average value of 149.9 ppb at 15:00 on 25 July 2013.

In contrast to NH₃, the highest monthly levels of SO₂ (7.0 ppb) and CO (885 ppb) were observed in June, which could be due to the open burning of agricultural waste (straw, cornstalk, and other crops) after harvest in the surrounding area. Previous studies have shown that the burning of crop residues is a crucial source of trace gases in the NCP during summer (Meng et al., 2009; Lin et al., 2011). The obvious impact of biomass burning was observed during 16–19 June 2013 period. As CO is mainly



emitted from anthropogenic sources such as the burning of biomass, the elevated CO concentrations (2529 ppb at 22:00 on 16 and 2488 ppb at 22:00 on 17 June) were observed. During this pollution episode, the average concentrations of NH₃, SO₂, NO_x, O₃ and CO were 42.6, 7.69, 18.8, 44.0 and 1092 ppb, respectively, which were about 1.2-1.5 times than the average values for the whole study period.

5 The monthly concentrations of SO₂, NO_x, and CO in July and August decreased because of rapid photochemical reduction, additional removal by rainfall, and excellent vertical mixing. For the secondary pollutant O₃, the highest monthly value was observed in June 2013, which was subject to strong influences from photochemical production, intense burning of biomass, and transport of regional pollution.

10 3.2.2 Diurnal variations of NH₃

The average diurnal variations of NH₃ during June to September 2013 are shown in Fig. 3. As indicated in Fig. 3a, NH₃ concentration maxima and minima were observed during 08:00–13:00 and 19:00–23:00, respectively. As for July, NH₃ concentrations showed a considerably more pronounced diurnal pattern with a maximum of 59.5 ppb at 08:00. The concentration of NH₃ gradually increased

15 during 00:00–03:00, remained relatively constant during 04:00–06:00, and then rapidly increased from 06:00 (beginning just after sunrise). After peaking at approximately 08:00, a decrease was observed until it reached the minimum of 29.8 ppb at 19:00.

The morning peak could be resulted from emissions from fertilised soils and plant stomata, evaporation of dew, and human sources, as well as mixing down of ammonia from the residual layer

20 (Bash et al., 2010; Ellis et al., 2011). Figure 4b reveals that the relative humidity (90%-89%) and temperature (21.5-22.1 °C) remained relatively constant before 06:00, but increased later in the morning. The increasing temperature can heat the earth's surface sufficiently to promote emissions from evaporation of morning dew and the soil and plant stomata, which may increase NH₃ concentrations in the morning. When the emission was occurring into a shallow nocturnal boundary layer, NH₃ increase

25 would be more prominent (Bash et al. 2010). In addition, the morning rise may also be due to the break up of the nocturnal boundary layer. When the vertical mixing begins, the downward mixing of the residual layer containing relatively higher NH₃ concentrations could lead to an increase of NH₃ in surface (Ellis et al., 2011).

NH₃ concentrations began to decrease in the afternoon as the daytime mixed layer further developed

30 with the high wind speed. The decreasing of NH₃ level from midnight to early morning might be



related to the relatively small amount of night time emissions under low temperature and the enhanced participation of NH_3 in particulate formation. Another simultaneous flux measurements and modeling studies are necessary for more robust explanation to the observed diurnal variations of NH_3 .

From Fig. 3a, it can be seen that the higher the NH_3 maximum is, the earlier it appears such as in 5 July. One reason for this might be the increased emissions of local agricultural NH_3 sources in July compared with those in June, August, and September; the resulting NH_3 peak in July occurred earlier than it did in the other months, particularly in September. Another possible cause for the earlier peak in August than in June involves meteorological factors such as the higher temperature, RH, and the lower wind speed in August. For instance, the air temperature increased from 07:00 reaching maximum value 10 (30.9 °C) at 15:00 in August, which was about of 3.3 °C higher than that in June, meanwhile the highest wind speed (2.73 m s⁻¹) at 13:00 in June was about of 1.0 m s⁻¹ higher than that in August.

Ambient NH_3 concentrations in an area of intensive crop production correlate positively with the air temperature. The maximum monthly value of NH_3 concentrations was consistent with the highest ambient temperature in July 2013. Predictably, the highest average diurnal amplitude of NH_3 (30.4 ppb) 15 was observed in July, with the lowest average diurnal amplitude of NH_3 (8.4 ppb) observed in September 2013.

3.3 Ambient ammonium aerosol

Secondary inorganic aerosols form from gas-phase precursors, which are mostly from anthropogenic activities such as industrial, agricultural, and motor vehicle emissions. Therefore, the major precursors 20 (NH_3 , SO_2 and NO_x) are responsible for the formation of particulate ammonium, sulphate, and nitrate.

The hourly NH_4^+ concentrations during 15 June–11 August 2013 ranged from 1.07 to 340.6 $\mu\text{g m}^{-3}$, with an average concentration of $19.8 \pm 33.2 \mu\text{g m}^{-3}$. Similar to NH_3 , the concentration of NH_4^+ also increased sharply after urea fertilisation, with the highest value (360.6 $\mu\text{g m}^{-3}$) observed at 09:00 on 28 July 2013. The highest monthly level of NH_4^+ appeared in July and lowest level appeared in June 2013.

25 The highest hourly SO_4^{2-} concentration (116.9 $\mu\text{g m}^{-3}$) was observed at 10:00 on 9 July and the second highest value was 111.4 $\mu\text{g m}^{-3}$ at 18:00 on 6 August, 2013. Despite the lower concentrations of SO_2 , higher SO_4^{2-} concentrations in summer were attributed to the higher temperature, O_3 concentration and solar radiation, which increase the photochemical activities, the atmospheric oxidation and markedly faster conversion of SO_2 to SO_4^{2-} . The average concentration of NO_3^- in $\text{PM}_{2.5}$ was 11.3 ± 9.1 30 $\mu\text{g m}^{-3}$, with the highest value of 109.3 $\mu\text{g m}^{-3}$ observed at 15:00 on 22 June, 2013. Since NH_4NO_3 is



volatile and tends to dissociate and remain in the gas phase in summer, the higher NO_3^- level detected may be due to abundant NH_3 to neutralize H_2SO_4 and HNO_3 .

Several pollution episodes of precursor gases, SO_4^{2-} , NO_3^- and NH_4^+ in $\text{PM}_{2.5}$ were observed during the study period. As shown in Fig. 4, the peak values of NH_3 , SO_2 and NO_x (76.3 ppb at 09:00, 14.9 ppb at 14:00 on and 42.2 ppb at 00:00 on 10 August, respectively) were observed, which were accompanied by the large increase in concentrations of SO_4^{2-} , NO_3^- and NH_4^+ during 7-11 August 2013. Due to the atmospheric conditions favoring the accumulation of pollutants, the concentrations of NH_4^+ , SO_4^{2-} and NO_3^- (24.8, 35.9 and $15.7 \mu\text{g m}^{-3}$, respectively) at 13:00 on 10 August were detected and higher compared with the average concentrations during 7-11 August 2013 by around 127%, 81% and 83%, respectively. These secondary ions concentrations had similar temporal distributions with slow accumulation and relatively rapid clearing under favourable meteorological conditions. There were good correlation between NH_3 with NH_4^+ , SO_4^{2-} and NO_3^- ($R=0.33$, 0.27 and 0.49 , respectively, with $P < 0.01$). This observation emphasizes the important role of NH_3 in the formation of secondary SO_4^{2-} , NO_3^- and NH_4^+ aerosols, which should be further explored to solve the current air pollution problems in NCP and other regions of the world.

During 7-11 August 2013, the relationships of the observed NH_4^+ versus those of SO_4^{2-} , the sum of SO_4^{2-} and NO_3^- and the sum of SO_4^{2-} , NO_3^- and Cl^- are also analyzed. It is known that $(\text{NH}_4)_2\text{SO}_4$ is preferentially formed and the least volatile, NH_4NO_3 is relatively volatile, while NH_4Cl is the most volatile. NH_4^+ is thought to be first associated with SO_4^{2-} , afterwards, the excess of NH_4^+ is with nitrate and chloride (Meng et al., 2015). It is noted that the correlation of NH_4^+ with the sum of SO_4^{2-} and NO_3^- ($R=0.91$, with $P < 0.01$) was better than that of NH_4^+ with SO_4^{2-} ($R=0.80$, with $P < 0.01$), suggesting that both SO_4^{2-} and NO_3^- were associated with NH_4^+ . Little different was found between the regression slopes of NH_4^+ with the sum of SO_4^{2-} and NO_3^- and the sum of SO_4^{2-} , NO_3^- and Cl^- due to the very low amount of NH_4Cl . In this study, NH_4^+ was enough to neutralize both SO_4^{2-} and NO_3^- , and likely to be in the form of $(\text{NH}_4)_2\text{SO}_4$, NH_4HSO_4 , and NH_4NO_3 .

The analysis of water-soluble ions in $\text{PM}_{2.5}$ at NCP rural site also indicated that biomass burning was a crucial source of aerosol species. This attribution is supported by the concentrations of K^+ in $\text{PM}_{2.5}$, an excellent indicator for biomass burning emission. The monthly concentrations of K^+ in $\text{PM}_{2.5}$ were 2.17, 1.62 and $0.98 \mu\text{g m}^{-3}$ in June, July and August, respectively, with the highest concentration in June 2013. During the period of 16–19 June, 2013, elevated concentrations of K^+ ($33.28 \mu\text{g m}^{-3}$ at



08:00 on 16 June), NH_4^+ ($33.28 \mu\text{g m}^{-3}$), SO_4^{2-} ($24.53 \mu\text{g m}^{-3}$), and NO_3^- ($29.79 \mu\text{g m}^{-3}$) were observed, which is consistent with the increase of CO , SO_2 , NO_x and NH_3 at the same time.

3.4 Relationship between ammonia and ammonium aerosol

The gas-to-particle conversion between NH_3 and NH_4^+ has been reported to be strongly affected by temperature, RH, radiation conditions, the concentration of primary acid gas, and other factors. In this study, NH_4^+ concentrations correlated significantly and positively with NH_3 concentrations ($R = 0.78$, $n=915$, $P < 0.01$), suggesting that NH_3 played an important precursor role in NH_4^+ in $\text{PM}_{2.5}$ formation.

The ratio of NH_3 to NH_x ($\text{NH}_3 + \text{NH}_4^+$) has been used to identify the source of NH_x and the relative contribution of NH_3 to NH_x deposition (Walker et al., 2004). A value higher than 0.5 signifies that NH_x is mainly from local NH_3 sources and that the dry deposition of NH_3 dominates the NH_x deposition. Robarge et al. (2002) reported that more than 70% of NH_x was in the form of NH_3 at an agricultural site in the South-eastern United States, and concluded that given a larger deposition velocity of ammonia compared with that of ammonium, a considerable fraction of NH_x could be deposited locally rather than be transported out of the region.

According to hourly average concentrations, the ratio of NH_3/NH_x varied from 0.22 to 0.97, with a mean ratio of 0.69 ± 0.14 , suggesting that NH_x was mainly influenced by local sources in summer 2013. It can also be inferred that NH_3 dry deposition could dominate NH_x deposition, while NH_4^+ was contributed to by both long-range transport and local formation.

3.4.1 Gas- to-particle conversion ratio of NH_3

Sulphate and nitrate oxidation ratios (SOR and NOR) are defined in literature to investigate SO_4^{2-} and NO_3^- formation and gas-particle transformation (Zhang et al., 2011). The average values of SOR and NOR were estimated to be 64% and 24% during the observation period at Gucheng, with SOR and NOR being higher than previous measurements (Zhou et al., 2009; Du et al., 2011; Zhang et al., 2011). Yao et al. (2002) pointed out an SOR lower than 10% under conditions of primary source emissions and higher than 10% when sulphate was mainly produced through the secondary transformation of SO_2 oxidation. The value of SOR reached to 70% in August 2013, indicating that the secondary transformation was very significant during summer at Gucheng.

To gain further insights into the transformation of NH_3 to NH_4^+ , the conversion ratio of ammonium (NHR) was investigated. NHR is a measure of the extent of transformation from NH_3 to NH_4^+ in areas with major local NH_3 sources. In this study, the average hourly values of NHR ranged from 3% to 77%,



with an average of 30% during summer 2013. The average NHR level in this study was higher than that observed at an urban site in Beijing (Meng et al., 2017), indicating that high NH_3 concentrations resulting from agricultural activities had a marked influence on the formation of ammonium. After applying fertilizer such as urea, NH_3 volatilization achieved the peak values, especially after the rainfall, which was in favour of the formation of NH_4^+ . To specifically explore the behaviour and chemical transformation, we analyzed in detail the episode during which the highest hourly NH_3 and NH_4^+ were observed.

Figure 5 illustrates the time series of the concentrations of air pollutants related to NH_4^+ formation and meteorological data on 27 to 31 July, 2013. NH_3 concentrations increased gradually from the afternoon of 27 July, and the obvious formation of NH_4^+ was also observed. In addition, during the night time (20:00 on 27-07:00 on 28 July), the average RH was 92% and the wind speed was 0.4 m s^{-1} , respectively, which may enhance the conversion of ammonia to ammonium via aqueous phase processes. As the rapid increase of solar radiation, the highest hourly value of NH_4^+ was observed at 09:00 on 28 July, and the corresponding NHR peaked (63%) at the same time.

NH_3 exhibited a maximum average concentration at 04:00 on 29 July, while NH_4^+ concentrations increased rapidly and remained high levels in the morning, with the NHR value rising to 53% at 09:00 on 29 July. Elevated NH_3 levels coincided with elevated NH_4^+ , indicating that NH_3 was the main factor promoting NH_4^+ formation.

Furthermore, on 30 July, the higher NH_4^+ concentration and NHR occurred around noon after NH_3 decreased, which is consistent with increasing solar radiation and O_3 concentration. This suggests that strong solar radiation intensity accelerated the photochemical formation of sulphuric acid or nitric acid, which subsequently reacted with NH_3 to form NH_4^+ . The increases in NHR coincided with those of NH_3 and O_3 concentrations and strong solar radiation intensity.

3.4.2 Diurnal patterns of NHR, SOR and NOR

Fig. 6 presents the diurnal patterns of NHR, SOR, NOR, gaseous precursors, and major water soluble ions, and meteorological factors. As a key species contributing to the oxidisation capacity of the atmosphere, O_3 can promote HNO_3 formation, affecting the conversion ratio of NH_3 . O_3 exhibited low levels in the morning and enhanced levels in the late afternoon. The lower morning concentrations may be due to the depositional loss of O_3 under stable atmospheric conditions in early morning hours, and the higher levels in the afternoon could be due to the photochemical production of O_3 . The NH_4^+



concentration started to increase at noon, reaching the maximum value ($15.8 \mu\text{g m}^{-3}$) at 18:00, with a diurnal difference of $3.6 \mu\text{g m}^{-3}$. This diurnal pattern may be due to a combination of high NH_3 concentrations, the intense solar radiation at noon, and the high oxidisation capacity of the atmosphere in the afternoon. A clear diurnal cycle of NHR with a peak of 48% was observed at 19:00, which is
5 consistent with the higher NH_4^+ and SO_4^{2-} concentrations and RH.

The SO_2 concentration showed a maximum at 09:00, with a secondary peak at 22:00. The concentration of SO_4^{2-} showed small peak at 13:00, 16:00, and 19:00, respectively, but no strong diurnal variation. SOR displayed a diurnal cycle with the highest value of 53% observed at 19:00 and the second highest level of 51% exhibited at 04:00. The maximum value of SO_4^{2-} coincide to O_3 and
10 SOR, which may due to the intense solar radiation and the high oxidization degree of the atmosphere.

As for the diurnal cycle of NO_x , a peak was observed at 06:00 when the mixing layer was stable, and a broad valley was observed in the daytime, which was likely due to a higher mixing layer and stronger photochemical conversion. During the night, NO_x concentrations increased again, resulting in the second maximum at 23:00. NO_3^- concentrations did not show profound diurnal variations, but slightly
15 higher values during the night time, probably because of the hydrolysis of dinitrogenpentoxide (N_2O_5) and the condensation of HNO_3 under the relatively low temperature. NOR displayed a diurnal pattern with a maximum of 34% at 14:00, which was likely related to photochemical reactions under the conditions of high O_3 concentrations and solar radiation.

3.5 The impact of air masses transport on the surface ammonia and ammonium

20 To identify the impact of long-range air transport on the surface air pollutants levels and secondary ions at Gucheng, the 72-h backward trajectories were calculated using the HYSPLIT 4.9 model.

As can be seen in Fig. 7, the Clusters 1, 2 and 3 represent relatively low and slow moving air parcels, with cluster 2 coming from northwest areas at the lowest transport height among the five clusters. The Cluster 4 and 5 represent air parcels mainly from the northwest.

25 The trajectories in Clusters 2 come from the local areas around Gucheng, and it was the most important cluster to the Gucheng site, contributing 56% of air masses. Based on the statistics, the number of trajectories in Cluster 1, 2 and 3 accounts to 88% of the all trajectories. As more than 80% air masses originated from or passing over the North China Plain region can influence the surface measurements at Gucheng, the observation results at Gucheng can well represent the regional changes
30 of atmospheric components in the North China Plain region.



Since the emission sources of pollutants are unevenly distributed in the areas surrounding the Gucheng site, air masses from different directions containing different levels of pollutants. The corresponding mean concentrations of NH_3 , SO_2 , NO_x , NH_4^+ , SO_4^{2-} and NO_3^- in $\text{PM}_{2.5}$ in different clusters of backward trajectories are also included in Table 2 in order to characterize the dependences of the pollutants concentrations on air masses.

Large differences in the concentrations of NH_3 , SO_2 , NO_x , NH_4^+ , SO_4^{2-} and NO_3^- in $\text{PM}_{2.5}$ existed among the different clusters, with cluster 2 corresponding to the highest NH_3 (48.9 ppb) and second highest NO_x , NH_4^+ and SO_4^{2-} (14.4 ppb, 17.5 $\mu\text{g m}^{-3}$ and 22.1 $\mu\text{g m}^{-3}$, respectively). The cluster 1 corresponds to highest SO_2 , NH_4^+ , SO_4^{2-} and NO_3^- (7.9 ppb, 22.3 $\mu\text{g m}^{-3}$, 22.6 $\mu\text{g m}^{-3}$ and 17.7 $\mu\text{g m}^{-3}$, respectively), the second highest NH_3 level (32.8 ppb). The cluster 3 had the highest NO_x level (15.1 ppb), the second highest SO_2 and NO_3^- (4.8 ppb and 11.8 $\mu\text{g m}^{-3}$, respectively), and had the third highest concentration of NH_3 , NH_4^+ and SO_4^{2-} levels (28.5 ppb, 14.6 $\mu\text{g m}^{-3}$, and 20.2 $\mu\text{g m}^{-3}$, respectively). Based on table 2, the lowest NH_3 , SO_2 , NO_x , NH_4^+ , SO_4^{2-} and NO_3^- levels were corresponding to clusters 5, which was expected to bring cleaner air masses into surface. As demonstrated by backward trajectory, more than half of the air masses during the sampling period from North China Plain region contributed to the atmospheric NH_3 variations, and both regional sources and long-distance transport from southeast played important roles in the observed ammonium aerosol at the rural site in the NCP.

4 Conclusions

Online measurements of NH_3 , trace gases, and water-soluble ions in $\text{PM}_{2.5}$ were conducted during May–September 2013 at a rural site in the NCP, where a large amount of ammonia was emitted because of agricultural activities. The average concentrations of NH_3 and NH_4^+ in $\text{PM}_{2.5}$ were 36.2 ± 56.4 ppb during 15 May–25 September, 2013, and 18.9 ± 33.2 $\mu\text{g m}^{-3}$ during 15 June–11 August, 2013, respectively; these are considerably higher than those reported at other sites in China, Europe and North American. Extremely high NH_3 and NH_4^+ concentrations were observed, which was attributed to high soil moisture level due to rainfall on these days following the urea application. Elevated NH_3 levels coincided with elevated NH_4^+ , indicating the contribution of atmospheric NH_3 to secondary inorganic aerosols during periods of agricultural activity. NH_3 contributed 69% to the total $\text{NH}_3+\text{NH}_4^+$ in summer, suggesting that NH_x was influenced by local sources and that NH_3 dry deposition could contribute a large part of the NH_x deposition.



The average conversion/oxidation ratio for NH_4^+ (NHR), SO_4^{2-} (SOR), and NO_3^- (NOR) were estimated to be 30%, 64%, and 24% in summer 2013, respectively. Results reveal that the concentrations of NH_3 , NH_4^+ , and NHR had clear diurnal variations during the observation period. The increased NH_3 concentrations mainly from fertilization, coincided with the prevailing meteorological conditions, including high relative humidity, degree of oxidisation, and low wind could promote the secondary transformation, resulting in higher hourly SOR, NOR and NHR. The back trajectory analysis indicates that the transport from the North China Plain region contributed for 56% of air mass with high NH_3 levels, meanwhile the long-distance transport from southeast accounted for 32% of air mass with high NH_4^+ , SO_4^{2-} and NO_3^- at the rural site in the NCP. NH_3 is currently not included in China's emission control policies of air pollution precursors, our findings highlight the important role of NH_3 in secondary inorganic aerosol formation and are expected to facilitate developing future NH_3 emission control policies for the North China Plain.

References

- 15 Aranibar, J. N. , Otter, L., Macko, S. A., Feral, C. J. W., Epstein, H. E., Dowty, P. R., Eckardt, F., Shugart, H. H., and Swap, R. J.: Nitrogen cycling in the soil plant system along a precipitation gradient in the Kalahari sands, *Glob. Chang. Biol.*, 10, 359-373, 2004.
- Bash, J. O., Walker, J. T., Katul, G. G., Jones, M. R., Nemitz, E., and Robarg, W. P.: Estimation of In-Canopy Ammonia Sources and Sinks in a Fertilized Zea mays Field, *Environ. Sci. Tech.*, 44, 1683-1689, 2010.
- 20 Behera, S. N., Betha, R., and Balasubramanian, R.: Insight into chemical coupling among acidic gases, ammonia and secondary inorganic aerosols, *Aerosol Air Qual. Res.*, 13, 1282-1296, 2013.
- Behera, S. N. and Sharma, M.: Investigating the potential role of ammonia in ion chemistry of fine particulate matter formation for an urban environment, *Sci. Total Environ.*, 408, 3569-3575, 2010.
- 25 Biswas, K.F., Ghauri, B. M. and Husain, L.: Gaseous and aerosol pollutants during fog and clear episodes in South Asian urban atmosphere, *Atmos. Environ.*, 42, 7775-7785, 2008.
- Burch, J. A. and Fox, R. H.: The effect of temperature and initial soil moisture content on the volatilization of ammonia from surface applied urea, *Soil Sci.*, 147, 311-318, 1989.
- Cao, J. J., Zhang, T., Chow, J. C., Watson, J. G., Wu, F., and Li, H.: Characterization of Atmospheric Ammonia over Xi'an, China, *Aerosol Air Qual. Res.*, 9, 277-289, 2009.
- 30



- Dong, W., Xing, J. and Wang, S.: Temporal and spatial distribution of anthropogenic ammonia emissions in China: 1994-2006, *Environ. Sci.*, 31, 1457-1463, 2010. (in Chinese).
- Du, H. H., Kong, L. D., Cheng, T. T., Chen, J. M., Du, J. F., Li, L., Xia, X. G., Leng, C. P., and Huang, G. H.: Insights into summertime haze pollution events over Shanghai based on online water soluble ionic composition of aerosols, *Atmos. Environ.*, 45, 5131–5137, 2011.
- 5 Ellis, R. A., Murphy, J. G., Markovic, M. Z., VandenBoer, T. C., Makar, P. A., Brook, J., and Mihele, C.: The influence of gas-particle partitioning and surface-atmosphere exchange on ammonia during BAQS-Met, *Atmos. Chem. Phys.*, 11, 133-145, 2011.
- Erismann, J. W. and Schaap, M.: The need for ammonia abatement with respect to secondary PM reductions in Europe, *Environ. Pollut.*, 129, 159-163, 2004.
- 10 Galloway, J. N., Aber, J. D., Erismann, J. W., Seitzinger, S. P., Howarth, R. W., Cowling, E. B., and Cosby, B. J.: The nitrogen cascade, *BioScience*, 53, 341-353, 2003.
- Gong, L. W., Lewicki, R., Griffin, R. J., Tittel, F. K., Lonsdale, C. R., Stevens, R. G., Pierce, J. R., Malloy, Q. G.J., Travis, S. A., Bobmanuel, L. M., Lefer, B. L., and Flynn, J. H.: Role of atmospheric ammonia in particulate matter formation in Houston during summertime, *Atmos. Environ.*, 77, 893-900, 2013.
- 15 Guo, S., Hu, M., Wang, Z. B., and Zhao, Y. L.: Size-resolved aerosol water-soluble ionic compositions in the summer of Beijing: implication of regional secondary formation, *Atmos. Chem. Phys.*, 10, 947-959, 2010.
- 20 Hassan, S. K., El-Abssawy, A. A., and Khoder, M. I.: Characteristics of gas-phase nitric acid and ammonium-nitrate-sulfate aerosol, and their gas-phase precursors in a suburban area in Cairo, Egypt, *Atmos. Pollut. Res.*, 4, 117-129, 2013.
- Hu, M., Wu, Z.J., Slanina, J., Lin, P., Liu, S., and Zeng, L. M.: Acidic gases, ammonia and water-soluble ions in $PM_{2.5}$ at a coastal site in the Pearl River Delta, China, *Atmos. Environ.*, 42, 6310-6320, 2008.
- 25 Hu, G. Y., Zhang, Y. M., Sun, J. Y., Zhang, L. M., Shen, X. J., Lin, W. L., and Yang, Y.: Variability, formation and acidity of water-soluble ions in $PM_{2.5}$, in Beijing based on the semi-continuous observations, *Atmos. Res.* 145-146: 1-11, 2014.
- Ianniello, A., Spataro, F., Esposito, G., Allegrini, I., Rantica, E., Ancora, M. P., Hu, M., and Zhu, T.: Occurrence of gas phase ammonia in the area of Beijing (China), *Atmos. Chem. Phys.*, 10,
- 30



- 9487-9503, 2010.
- Krupa, S. V.: Effects of atmospheric ammonia (NH_3) on terrestrial vegetation: A review. *Environ. Pollut.*, 124, 179-221, 2003.
- Lei, H. and Wuebbles, D.J.: Chemical competition in nitrate and sulfate formations and its effect on air
5 quality, *Atmos. Environ.*, 80, 472-477, 2013.
- Li, Y., Schwandner, F. M., Sewell, H. J., Zivkovich, A., Tigges, M., Raja, S., Holcomb, S., Molenaar,
J.V., Sherman, L., Archuleta, C., Lee, T., and Collett, J. L.: Observations of ammonia, nitric acid,
and fine particles in a rural gas production region, *Atmos. Environ.*, 83, 80-89, 2014.
- Lin, Y. C., Cheng, M. T., Ting, W. Y., and Yeh, C. R.: Characteristics of gaseous HNO_2 , HNO_3 , NH_3
10 and particulate ammonium nitrate in an urban city of central Taiwan, *Atmos. Environ.*, 40,
4725-4733, 2006.
- Lin, W., Xu, X., and Zhang, X.: Characteristics of gaseous pollutants at Gucheng, a rural site southwest
of Beijing, *J. Geophys. Res.*, 114, 10339, 2009.
- Lin, W., Xu, X., Ge, B., and Liu, X.: Gaseous pollutants in Beijing urban area during the heating period
15 2007-2008: variability, sources, meteorological and chemical impacts, *Atmos. Chem. Phys.*, 11,
8157-8170, 2011.
- Liu, X. J., Zhang, Y., Han, W.X., Tang, A. H., Shen, J. L., Cui, Z. L., Peter, V., Jan, W. E., Keith, G.,
Peter, C., Andreas, F., and Zhang, F. S.: Enhanced nitrogen deposition over China, *Nature*, 28,
459-463, 2013.
- 20 Luo, X. S., Liu, P., Tang, A. H., Liu, J. Y., Zong, X. Y., Zhang, Q., Kou, C. L., Zhang, L. J., Fowler, D.,
Fangmeier, A., Christie, P., Zhang, F. S., and Liu, X. J.: An evaluation of atmospheric Nr pollution
and deposition in North China after the Beijing Olympics, *Atmos. Environ.*, 74, 209-216, 2013.
- Makkonen, U., Virkkula, A., Mäntykenttä, J., Hakola, H., Keronen, P., Vakkari, V., and Aalto, P. P.:
Semi-continuous gas and inorganic aerosol measurements at a Finnish urban site: comparisons with
25 filters, nitrogen in aerosol and gas phases, and aerosol acidity, *Atmos. Chem. Phys.*, 12, 5617-5631,
2012.
- Meng, Z. Y., Lin, W. L., Jiang, X. M., Yan, P., Wang, Y., Zhang, Y. M., Jia, X. F., and Yu, X. L.:
Characteristics of atmospheric ammonia over Beijing, China, *Atmos. Chem. Phys.*, 11, 6139-6151,
2011.
- 30 Meng, Z. Y., Lin, W. L., Zhang, R. J., Han, Z. W. and Jiang, X. F.: Summertime ambient ammonia and



- its effects on ammonium aerosol in urban Beijing, China, *Sci. Total Environ.*, 578, 2185-2201, 2016.
- Meng, Z. Y., Xie, Y. L., Jia, S. H., Zhang, R., Lin, W. L., Xu, X. B., and Yang W.: The characteristics of atmospheric ammonia at Gucheng, a Rural Site in the North China Plain in summer 2013, *J. applied. meteor. sci.*, 26, 141-150, 2015. (in Chinese).
- 5 Meng, Z. Y., Xu, X. B., Yan, P., Ding, G. A., Tang, J., Lin, W. L., Xu, X. D., and Wang, S. F.: Characteristics of trace gaseous pollutants at a regional background station in Northern China, *Atmos. Chem. Phys.*, 9, 927-936, 2009.
- Meng, Z. Y., Zhang, R. J., Lin, W. L., Jia, X. F., Yu, X. M., Yu, X. L., and Wang, G. H.: Seasonal variation of ammonia and ammonium aerosol at a background station in the Yangtze River Delta 10 Region, China, *Aerosol Air Qual. Res.*, 3, 756-766, 2014.
- Park, R. S., Lee, S., Shin, S. K. and Song, C. H.: Contribution of ammonium nitrate to aerosol optical depth and direct radiative forcing by aerosols over East Asia, *Atmos. Chem. Phys.*, 14, 2185-2201, 2014.
- 15 Plessow, K., Spindler, G., Zimmermann, F. and Matschullat, J.: Seasonal variations and interactions of N-containing gases and particles over a coniferous forest, Saxony, Germany, *Atmos. Environ.*, 39, 6995-7007, 2005.
- Reche, C., Viana, M., Karanasiou, A., Cusack, M., Alastuey, A., Artiñano, B., Revuelta, M., López-Mahía, P., Blanco-Heras, G., Rodríguez, S., Sánchez de la Campa, A., Fernández-Camacho, 20 R., González-Castanedo, Y., Mantilla, E., Tang, S., and Querol, X.: Urban NH₃ levels and sources in six major Spanish cities, *Chemosphere*, 119, 769-777, 2015.
- Reynold, C.M. and Wolf, D.: Effect of soil moisture and air relative humidity on ammonia volatilization from surface-applied urea, *Soil Sci.*, 143, 144-152, 1987.
- Robarge, W. P., Walker, J. T., McCulloch, R. B., and Murray, G.: Atmospheric concentrations of 25 ammonia and ammonium at an agricultural site in the southeast United States, *Atmos. Environ.*, 36, 16611-1674, 2002.
- Roelle, P. A. and Aneja, V. P.: Characterization of ammonia emissions from soils in the upper coastal plain, North Carolina, *Atmos. Environ.* 36, 1087-1097, 2002.
- Schaap, M., Otjes, R. P. and Weijers, E. P.: Illustrating the benefit of using hourly monitoring data on 30 secondary inorganic aerosol and its precursors for model evaluation, *Atmos. Chem. Phys.*, 11,



- 11041-11053, 2011.
- Shen, J. L., Liu, X. J., Zhang, Y., Fangmeier, A., Goulding, K., and Zhang, F. S.: Atmospheric ammonia and particulate ammonium from agricultural sources in the North China Plain, *Atmos. Environ.*, 45, 5033-5041, 2011.
- 5 Walker, J. T., Robarge, W. P., Shendrikar, A., and Kimball, H.: Inorganic PM_{2.5} at a U.S. agricultural site, *Environ. Pollut.*, 139, 258-271, 2006.
- Walker, J. T., Whittall, D. R., Robarge, W., and Paerl, H. W.: Ambient ammonia and ammonium aerosol across a region of variable ammonia emission density., *Atmos. Environ.*, 38, 1235-1246, 2004.
- Wang, S. S., Nan, J.L., Shi, C. Z., Fu, Q. Y., Gao, S., Wang, D. F., Cui, H. X., Alfonso, S. L., and Zhou,
10 B.: Atmospheric ammonia and its impacts on regional air quality over the megacity of Shanghai, China. *Sci. Rep.*, 5, 15842, 2015.
- Wang, T., Nie, W., Gao, J., Xue, L. K., Gao, X. M., Wang, X. F., Qiu, J., Poon, C. N., Meinardi, S., Blake, D., Wang, S. L., Ding, A. J., Chai, F. H., Zhang, Q. Z., and Wang, W. X.: Air quality during the 2008 Beijing Olympics: secondary pollutants and regional impact, *Atmos. Chem. Phys.*, 10,
15 7603-7615, 2010.
- Wei, L. F., Duan, J. C., Tan, J. H., Ma, Y. L., He, K. B., Wang, S. X., Huang, X. F., and Zhang, Y. X.: Gas-to-particle conversion of atmospheric ammonia and sampling artifacts of ammonia in spring of Beijing, *Sci. China Earth Sci.*, 58, 345-355, 2015.
- Yao, X. H., Ling, T. Y., Fang, M. and Chan, C. K.: Comparison of thermodynamic predictions for in
20 situ pH in PM_{2.5}, *Atmos. Environ.* 40, 2835-2844, 2006.
- Yao, X.H., Chak, K.C., Fang, M., Cadle, S., Chan, T., Mulawa, P., He, K.B., and Ye, B.M.: The water-soluble ionic composition of PM_{2.5} in Shanghai and Beijing, China, *Atmos. Environ.* 36, 4223-4234, 2002.
- Ye, X. N., Ma, Z., Zhang, J.C., Du, H. H., Chen, J. M., Chen, H., Yang, X., Gao, W., and Geng, F. H.:
25 Important role of ammonia on haze formation in Shanghai, *Environ. Res. Lett.*, 6, 024019, 2011.
- Zhang, Y., Dore, A. J., Ma, L., Liu, X. J., Ma, W. Q., Cape, J. N., and Zhang, F. S.: Agricultural ammonia emissions inventory and spatial distribution in the North China Plain, *Environ. Pollut.*, 158, 490-501, 2010.
- Zhang, T., Cao, J., Tie, X., Shen, Z., Liu, S., Ding, H., Han, Y., Wang, G., Ho, K., Qiang, J., and Li, W.:
30 Water-soluble ions in atmospheric aerosols measured in Xi'an, China: Seasonal variations and



sources, Atmos. Res. 102, 110-119, 2011.

Zhou, Y., Wang, T., Gao, X. M., Xue, L. K., Wang, X. F., Wang, Z., Gao, J., Zhang, Q. Z., and Wang, W. X.: Continuous observations of water-soluble ions in PM_{2.5} at Mount Tai (1534 m a.s.l.) in central-eastern China, J. Atmos. Chem. 64, 107-127, 2009.

5

Acknowledgements

This work was supported by the National Natural Science Foundation of China (2137716 and 41330422), the Environmental Protection Public Welfare Scientific Research Project, Ministry of Environmental Protection of the People's Republic of China (grant No. 201509001, 201509002-04 and 10 201309009), and the China Special Fund for Meteorological Research in the Public Interest (GYHY201206015). The authors would like to thank Professor Xiangde Xu and Yu Song for their helpful support and suggestions. The authors would like to thank Professor Yaqiang Wang for providing NH₃ emission data and the plotting helps of Chao He.



Table Captions

Table 1. The comparisons of the concentration of trace gases (ppb) and water-soluble ions in $PM_{2.5}$ ($\mu\text{g m}^{-3}$) at Gucheng with other researches.

Table 2. Occurrence frequency and mean values of NH_3 , other trace gases and water-soluble ions in
5 $PM_{2.5}$ for each type of air masses arriving at Gucheng during summer 2013.

Figure Captions

Figure 1. Sampling location in the North China Plain with emission distributions of NH_3 for the year
2012 from the multi-resolution emission inventory of China (<http://meicmodel.org/index.html>).

10 Figure 2. Time series of hourly data of NH_3 , other trace gases and meteorological parameters measured
during the sampling period.

Figure 3. Diurnal variation (a) NH_3 and (b) meteorological parameters during the sampling period.

Figure 4. Hourly concentrations of precursor gas and ionic species measured in the pollution episode
during 7–11 August 2013.

15 Figure 5. Time series of the concentrations of air pollutants related to NH_4^+ formation and
meteorological data on 27 to 31 July, 2013.

Figure 6. Diurnal variation of NHR, SOR, NOR, gaseous precursors, major water soluble ions, and
meteorological factors in summer 2013.

Figure 7. 72-h backward trajectories for 100 m above ground level at Gucheng during sampling period
20 2013.



Table 1. The comparisons of the concentration of trace gases (ppb) and water-soluble ions in $PM_{2.5}$ ($\mu\text{g m}^{-3}$) at Gucheng with other researches.

Location	Type	Period	NH ₃	SO ₂	NO _x	NH ₄ ⁺	SO ₄ ²⁻	NO ₃ ⁻	Reference
Gucheng, China	Rural	May.-Sept. 2013	36.2±56.4	5.0±6.5	15.4±9.3	19.8±33.2	20.5±13.6	11.3±9.1	This study
Shangdianzi, China	Rural	Jun.2008-Dec.2009	10.4±8.1	5.9±4.6	12.0±6.8	7.03±7.76	15.0±15.7	11.6±11.4	Meng et al. 2014
Beijing, China	Rural	Aug.2006-Jul.2007	21.1±10.5	–	37.8±11.6	8.8±6.7	22.4±16.2	15.1±11.4	Shen et al. 2011
Lin'an, China	Rural	Sept.2009-Dec.2010	16.5±11.2	6.4±4.2	10.8±5.2	4.3±3.5	9.6±6.1	7.3±7.5	Meng et al. 2014
Guangzhou, China	Rural	Oct.-Nov. 2004	10.5	21.2	–	9.2	24.1	7.2	Hu et al, 2008
Hong Kong, China	Urban	Autumn 2000	3	–	–	2.4	9	1	Yao et al. 2006
Taichung, Taiwan	Urban	Jan.-Dec. 2002	12.2±4.31	–	–	4.6±2.0	15±8.7	6.0±4.0	Lin et al. 2006
Lahore, Pakistan	Urban	Dec.2005-Feb.2006	72.1	7.4	–	16.1	19.2	18.9	Biswas et al, 2008
Colonelganj, India	Urban	Summer 2007	41.3±10.5	6.95±1.99	33.8±8.56	18.4±4.7	27.8±7.6	29.2±7.5	Behera et al. 2010
Singapore	Urban	Sep.-Nov. 2011	3.6	8.3	–	1.76	4.41	1.29	Behera et al. 2013
Oberbärenburg, Germany	Forest	Oct.2001-Apr.2003	0.69	2.24	–	1.55	3.07	2.22	Plessow et al, 2005
Netherlands	Rural	Aug. 2007 and 2008	12.9	0.5	–	2.4	3.1	5.9	Schaap et al. 2011
Helsinki, Finnish	Urban	Spring 2010	0.40±0.59	0.29±0.38	–	0.46±0.50	1.64±1.08	1.40±2.04	Makkonen et al. 2012
Cairo, Egypt	Suburban	Summer 2009	64.7	5.59	28.7	7.5	28	4.2	Hassan et al. 2013
Clinton, USA	Agricultural	Jan.1999-Dec.2000	8	1.5	–	1.76	4.22	2.05	Walker et al. 2006
Houston, USA	Urban	Aug. 2010	3.0±2.5	–	–	0.5±1.0	4.5±4.3	0.3±0.2	Gong et al, 2013
Wyoming, USA	Rural	Dec.2006-Dec.2011	0.24	–	–	0.26	0.48	0.32	Li et al. 2014



Table 2. Occurrence frequency and mean values of NH_3 , other trace gases (ppb) and ionic species in $\text{PM}_{2.5}$ ($\mu\text{g m}^{-3}$) for each type of air masses arriving at Gucheng in summer 2013.

Air mass	Ratio(%)	NH_3	SO_2	NO_x	NH_4^+	SO_4^{2-}	NO_3^-
Clusters 1	15	32.8	7.9	14.0	22.3	22.6	17.7
Clusters 2	56	48.9	3.7	14.4	17.5	22.1	10.3
Clusters 3	17	28.5	4.8	15.1	14.6	20.2	11.8
Clusters 4	10	23.4	2.4	12.8	12.9	15.3	7.2
Clusters 5	3	16.3	0.6	9.4	7.5	8.1	5.0

5

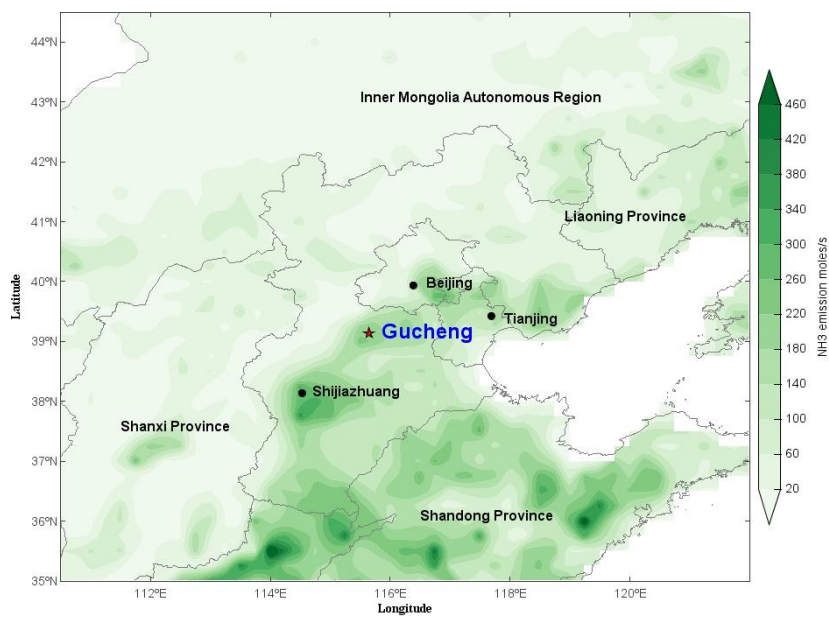


Figure 1. Sampling location in the North China Plain with emission distributions of NH_3 for the year 2012 from the multi-resolution emission inventory of China (<http://meicmodel.org/index.html>).

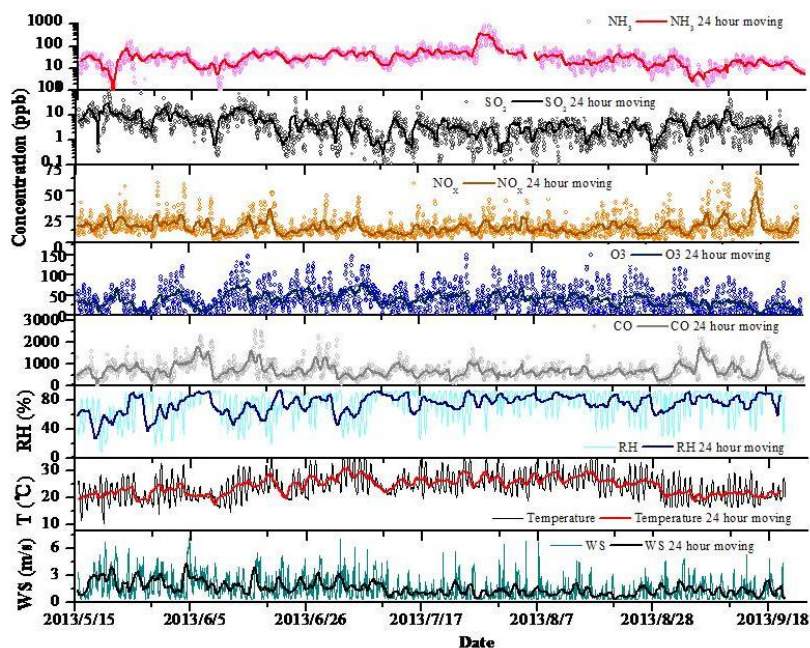


Figure 2. Time series of hourly data of NH_3 , other trace gases and meteorological parameters measured during the sampling period.

5

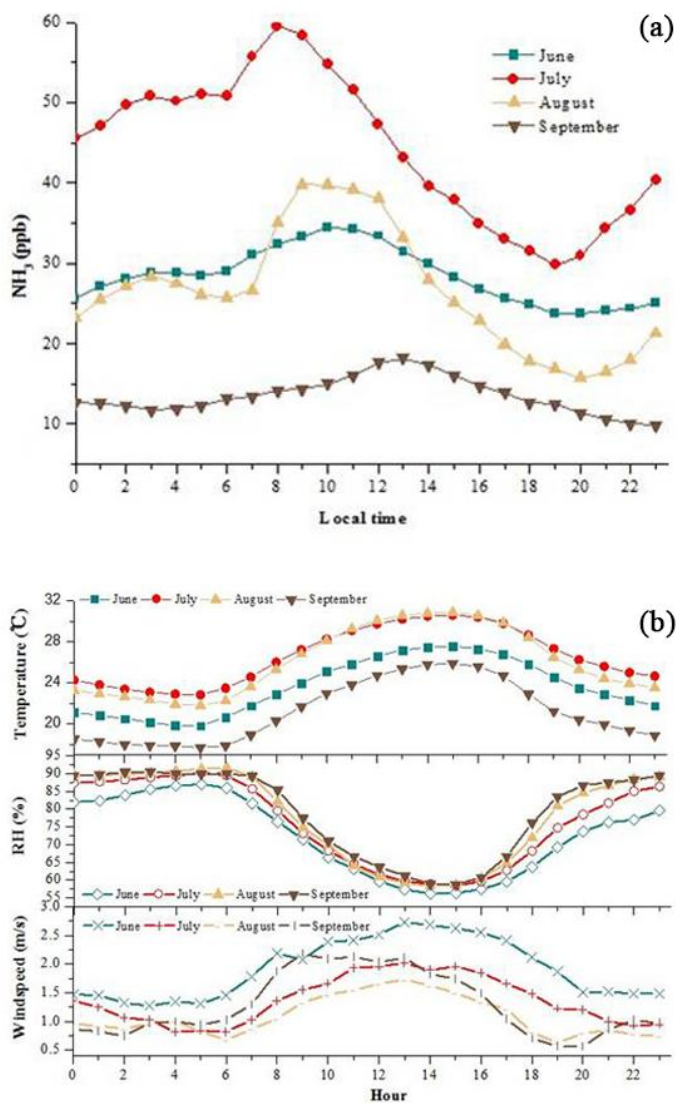


Figure 3. Diurnal variation (a) NH_3 and (b) meteorological parameters during the sampling period.

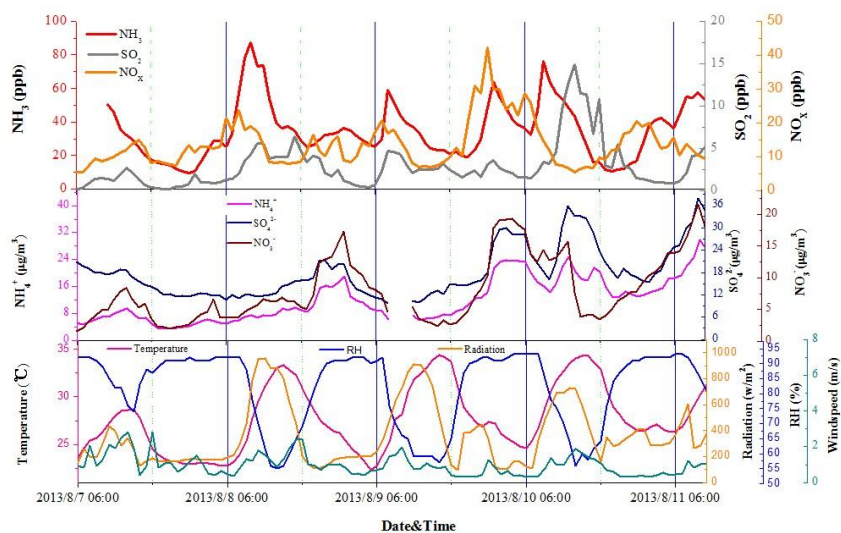


Figure 4. Hourly concentrations of precursor gas and ionic species measured in the pollution episode during 7–11 August 2013.

5

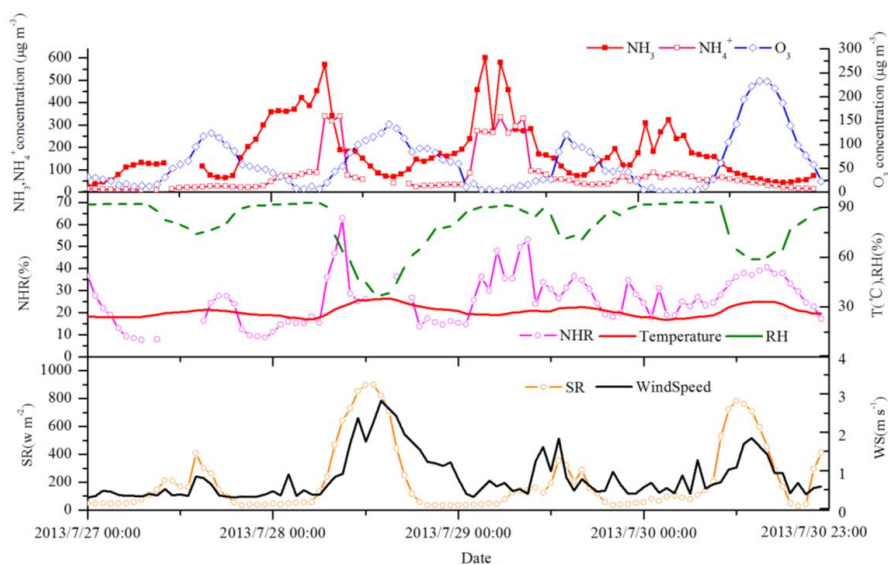


Figure 5. Time series of the concentrations of air pollutants related to NH_4^+ formation and meteorological data on 27 to 31 July, 2013.

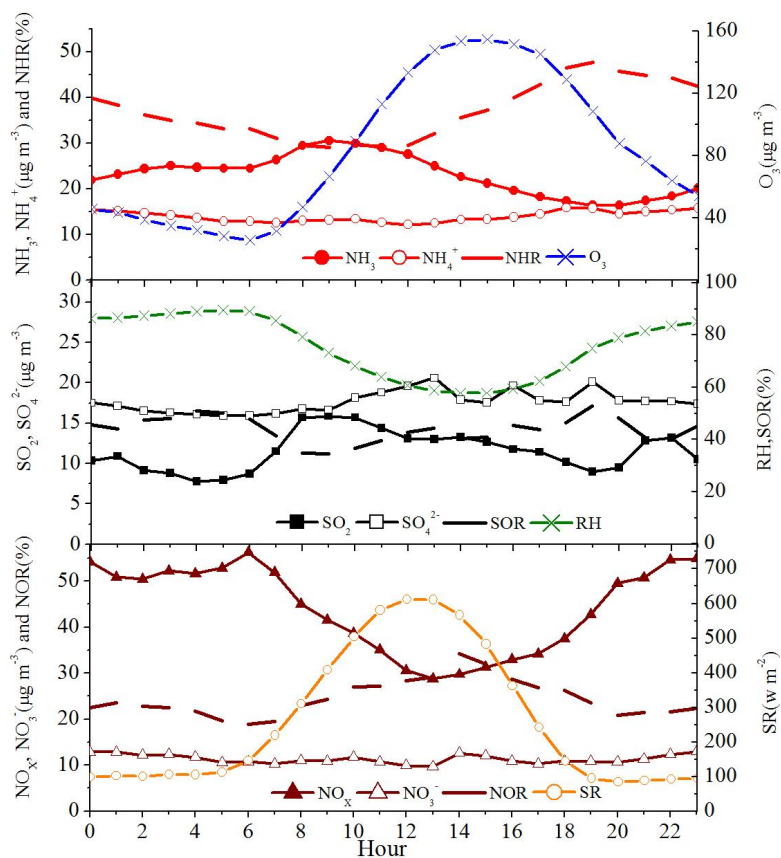


Figure 6. Diurnal variation of NHR, SOR, NOR, gaseous precursors, major water soluble ions, and meteorological factors in summer 2013.

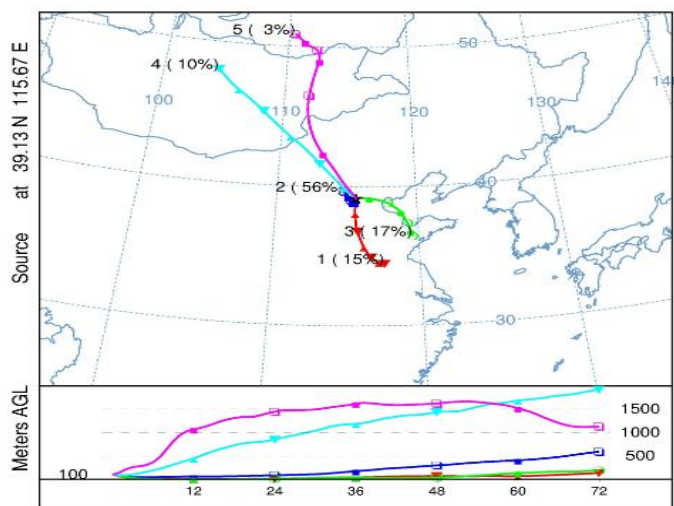


Figure 7. 72-h backward trajectories for 100 m above ground level at Gucheng during sampling period 2013.